Contents lists available at SciVerse ScienceDirect

ISPRS Journal of Photogrammetry and Remote Sensing

journal homepage: www.elsevier.com/locate/isprsjprs
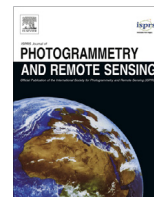
3-D voxel-based solid modeling of a broad-leaved tree for accurate volume estimation using portable scanning lidar

Fumiki Hosoi, Yohei Nakai, Kenji Omasa *

School of Agricultural and Life Sciences, The University of Tokyo, Yayoi 1-1-1, Bunkyo-ku, Tokyo 113-8657, Japan

ARTICLE INFO

ABSTRACT

We developed a method to produce a 3-D voxel-based solid model of a tree based on portable scanning lidar data for accurate estimation of the volume of the woody material. First, we obtained lidar measurements with a high laser pulse density from several measurement positions around the target, a Japanese zelkova tree. Next, we converted lidar-derived point-cloud data for the target into voxels. The voxel size was 0.5 cm × 0.5 cm × 0.5 cm. Then, we used differences in the spatial distribution of voxels to separate the stem and large branches (diameter > 1 cm) from small branches (diameter $\leqslant$ 1 cm). We classified the voxels into sets corresponding to the stem and to each large branch and then interpolated voxels to fill out their surfaces and their interiors. We then merged the stem and large branches with the small branches. The resultant solid model of the entire tree was composed of consecutive voxels that filled the outer surface and the interior of the stem and large branches, and a cloud of voxels equivalent to small branches that were discretely scattered in mainly the upper part of the target. Using this model, we estimated the woody material volume by counting the number of voxels in each part and multiplying the number of voxels by the unit voxel volume (0.13 cm^3). The percentage error of the volume of the stem and part of a large branch was 0.5%. The estimation error of a certain part of the small branches was 34.0%.

1. Introduction

Trees have important functional roles, including the cycling of materials and energy through photosynthesis and transpiration, the maintenance of microclimates, and the provision of habitats for various species (Jones, 1992; Larcher, 2001; Monteith, 1973). To understand the relationship between these functions and structure, many structural parameters, including height, stem diameter, leaf area density, volume, and biomass, have been measured by a variety of methods (Bragg, 2008; Norman and Campbell, 1989; Schnitzer et al., 2006). Recently, the importance of estimating tree volume or biomass for studies of global climate change has been recognized, because terrestrial vegetation is a major carbon storage pool and the carbon stock contained in tree canopies can be determined from their volume or biomass by using conversion factors. Thus, a method for accurate determination of the volume or biomass of trees is needed to determine the global carbon budget.

The most accurate method of estimating the volume or biomass of trees is to physically sample it (i.e., direct measurement). However, this method is not practical for most field research because it is both labor-intensive and destructive. Alternatively, satellite-based sensors such as the Landsat Enhanced Thematic Mapper, Synthetic-Aperture Radar (SAR), and the MODerate-Resolution Imaging Spectroradiometer (MODIS) have been used to estimate tree volume or biomass (le Maire et al., 2011; Maselli and Marta, 2006; Neumann et al., 2012). Although these sensors are suitable for regional-scale estimation, their resolution and accuracy are insufficient to provide detailed and accurate volume estimates at the individual-tree scale.

Recently, light detection and ranging (lidar) with laser scanners has emerged as a powerful active sensing tool for direct 3-D measurement of tree shapes and structures (Brandtberg et al., 2003; Côté et al., 2009; Holmgren and Persson, 2004; Hosoi et al., 2010; Hosoi and Omasa, 2006, 2007, 2009, 2012; Hopkinson et al., 2004; Hyyppä et al., 2001; Kaartinen et al., 2012; Lefsky and McHale, 2008; Lefsky et al., 2002; Means et al., 1999; Næsset et al., 2004; Omasa et al., 2000, 2002, 2003, 2007, 2008; Zhao et al., 2011). Lidar provides accurate 3-D information about trees by measuring the distance between the sensor and the target. Large-footprint airborne lidar systems can cover a wide expanse

* Corresponding author. Tel.: +81 3 5841 5340; fax: +81 3 5841 8175.
  E-mail address: aomasa@mail.ecc.u-tokyo.ac.jp (K. Omasa).

of a forest canopy, allowing the volume or biomass to be estimated by analyzing the waveforms of the returned laser pulses (Lefsky et al., 2002; Means et al., 1999). However, the image resolution of such systems is not fine enough for estimates at the scale of the individual tree. In contrast, small-footprint airborne lidar systems can cover a larger forest region with a fine enough resolution and sufficient accuracy for individual-tree-scale estimates. The volume or biomass of individual trees can be estimated from high-resolution images obtained by such lidar systems with high pulse repetition frequency through the application of allometric equations that relate the lidar-derived structural parameters to volume or biomass (Hyyppä et al., 2001; Næsset et al., 2004; Omasa et al., 2003, 2007). Portable on-ground scanning lidar systems have also been used for tree structural measurements (Côté et al., 2009, 2011; Dassot et al., 2011; Delagrange and Rochon, 2011; Hosoi and Omasa, 2006; Yao et al., 2011). The portability of such systems and their ability to efficiently collect data with very fine spatial resolution and accuracy (sub-millimeter to a few centimeters; Omasa et al., 2007) are advantageous for tree measurements on the ground. These systems can be used as an alternative to conventional in situ measurements of tree structure on the ground. Although the area covered by on-ground systems is not as large as that of airborne lidar systems, recent advances in lidar technology have increased the measurable range of portable systems to several hundred to a thousand meters with a range accuracy of better than 1 cm (Pirotti et al., 2013). Thus, portable scanning lidar systems are regarded as useful tools for ground-based plot-level tree measurements. Tree structural parameters such as height and diameter at breast height (DBH) have been extracted from 3-D point cloud images obtained by portable scanning lidar systems and used along with allometric equations (equations that establish quantitative relationships between key structural parameters of trees and other properties) to estimate volume or biomass (Hopkinson et al., 2004; Ku et al., 2012; Omasa et al., 2002; Yao et al., 2011). This method facilitates the estimation of volume or biomass without complex post-processing of the acquired data, but allometric equations are still required. In addition, allometric equations can only give a representative estimate based on the structural parameters, whereas shape and structure vary among individual trees. Thus, volume and biomass can vary among trees even though the structural parameters (e.g., height, DBH) input into the allometric equations have the same values. This limitation reduces the accuracy of volume and biomass estimates obtained by using the same allometric equations for all individuals of a species.

Portable scanning lidar systems can capture the complex shape and structure of individual trees as a detailed 3-D point-cloud image. Thus, 3-D tree models faithfully reproduced from the lidar-derived 3-D point-cloud image can be used to estimate the volume of trees without using allometric equations. Several 3-D tree modeling techniques have been employed for the estimation of individual tree volume and other structural properties from portable scanning lidar data (reviewed by Dassot et al., 2011). For example, modeling methods that extract the skeleton of a tree from 3-D point cloud data obtained by portable scanning lidar systems have been used to reconstruct tree architecture (Bucksch and Lindenbergh, 2008; Côté et al., 2009, 2011; Delagrange and Rochon, 2011). Côté et al. (2009, 2011) used such a modeling method to construct 3-D tree models that faithfully reflected the structural and radiative properties of the measured trees. In this modeling, the authors aimed to minimize the occlusion effect (that is, the lack of 3-D point cloud data for parts occluded by other branches, surrounding trees, and understory) which causes estimates of tree structural properties to be inaccurate (Côté et al., 2009, 2011; Dassot et al., 2011; Delagrange and Rochon, 2011; Hosoi and Omasa, 2007). Côté et al. (2009, 2011) considered their methodology to be relatively insensitive to the occlusion effect. Although they also used their model for volume

estimation, the accuracy of their estimates is not clear because they did not use field data to validate the estimation method. Using a method different from the tree skeleton extraction method, Omasa et al. (2008) produced 3-D polygonal surface models of individual tree canopies from portable scanning lidar data in conjunction with airborne scanning lidar data. Although they were able to estimate the volume of a part of the stem by this polygonization process, it was difficult to apply the process to the surfaces of stems and branches with complex shapes. Thus, the method could not be used to estimate the volume of the whole tree. Another approach to 3-D tree modeling based on lidar-derived point-cloud data is voxel representation (Hosoi and Omasa, 2006; Lefsky and McHale, 2008; Schilling et al., 2012; Vonderach et al., 2012). Hosoi and Omasa (2006) recently proposed a voxel-based method of 3-D modeling that uses high-resolution portable scanning lidar data (Voxel-based Canopy Profiling method). In this method, lidar data points are converted into voxel elements in a 3-D voxel array to faithfully reproduce the canopy as a voxel model. Although this method has been used for estimating vertical leaf area density profiles rather than for volume estimation, several studies have proved the ability of a voxel-based method to accurately estimate tree structural parameters (Hosoi and Omasa, 2006, 2007, 2009, 2012; Hosoi et al., 2010; Omasa et al., 2007). Lefsky and McHale (2008) also estimated tree volume in an urban area by 3-D voxel-based modeling using portable scanning lidar data. However, since their method approximates the shapes of stems and large branches as cylinders, it might not accurately reproduce their real shapes. In addition, Lefsky and McHale (2008) did not model small, very thin branches, which are a major canopy component, and thus the volumes of the small branches were not estimated. Moreover, because they did not compare the estimated volume with the actual measured volume, the accuracy of the method is uncertain. Therefore, accurate tree volume estimation by 3-D tree modeling is still under development.

In the present study, we propose a novel approach to 3-D tree modeling that enables tree volume to be accurately estimated from portable scanning lidar data. We validate the accuracy of the volume estimates obtained with the model by comparing them with the actual measured volumes.

2. Materials and methods

2.1. Study site

The study was carried out in a mixed plantation in Ibaraki Prefecture, 40 km northeast of central Metropolitan Tokyo, Japan. The dominant tree species are Japanese cedar (Cryptomeria japonica [L.f.] D. Don), Japanese red pine (Pinus densiflora Siebold & Zuccarini), ginkgo (Ginkgo biloba Linnaeus), and Japanese zelkova (Zelkova serrata [Thunberg] Makino). The understory includes grasses, forbs, and young evergreen trees such as Camellia japonica Linnaeus, Ilex integra Thunberg, and Ternstroemia gymnanthera Sprague. Tree density in the study area was about 600 trees per hectare. We established a 32 m^2 (4 m × 8 m) measurement plot at the site and chose a Japanese zelkova tree (height, 14 m; DBH, 0.25 m) within the plot for measurement. We established a relatively narrow plot and examined only one tree species to establish the basic processes used in the present modeling approach. Japanese zelkova is a medium to large deciduous tree, and its branches are numerous, usually ascending strongly from a short trunk to form a high domed crown (MobileReference, 2009). The complicated branch structure makes the zelkova tree an ideal species for model testing because the present method was designed to offer accurate volume estimation of even a complicated tree. Poles were placed at each corner of the measurement plot and scanned together with the target tree. From the positions of the poles in

the point cloud image, laser returns from the targeted zelkova tree could be identified. Hosoi and Omasa (2007) previously described the details of the measurement plot and the Japanese zelkova tree.

2.2. Portable ground-based scanning lidar measurements

In this study, only the volume of woody material, in the form of stems and branches, was quantified, because the method to estimate the quantity of leaves (i.e., leaf area density or leaf area index) has been already reported (Hosoi and Omasa, 2006, 2007, 2009, 2012; Hosoi et al., 2010; Omasa et al., 2007). Thus, the measurements were made in January 2010, during leaf-off conditions, with a portable ground-based scanning lidar system (LPM-25HA, RIEGL, Austria). This portable lidar system can obtain the distance to the surface of an object between 2 and 60 m from the sensor by measuring the time elapsed between the emitted and returned laser pulses (the "time of flight" method). A rotating mount driven by built-in stepper motors panned and tilted the lidar head with 0.009° accuracy, and the distance to each sample point was computed with an accuracy of ±8 mm. The target was scanned from six surrounding positions (similar to the previous setting described by Hosoi and Omasa, 2007). The central scan angle of the laser beams from the zenith was 57.8°, and the average distance of the lidar sensor from the targeted zelkova tree was about 10 m. The mean laser beam diameter and mean laser beam pitch (i.e., the mean of the distances between the centers of adjacent laser beams) in a plane perpendicular to the direction of the laser beam were both 12 mm at the distance of the target. This pitch value indicates that the laser pulse density (i.e., the number of incident laser pulses per unit area of a plane perpendicular to the direction of the laser pulse) was high.

2.3. Direct measurement of the tree volume

Immediately following the lidar data collection, we directly measured the volumes of the stem, part of a large branch, and some of the small branches. In this study, we defined branches with a diameter of more than 1 cm as "large branches" and all others as "small branches," because 1 cm is the approximate spatial resolution of the lidar system. First, we chose a continuous part of the target tree that included the stem and part of a large branch (as illustrated in the results section) for direct measurement. Next, we obtained clay molds of the outer shape of 0.30-m-long sections of the stem and branch between heights of 0.00 and 7.80 m at intervals of 0.30 m by pressing oil-based clay around each section. Then, we carefully removed the mold by making two cuts, longitudinally along the stem or the large branch, to retain the outer shape of that section. The mold was sufficiently thick (about 5 cm) to prevent deformation; thus, it preserved the outer shape of the stem or branch. We then photographed the inside of the clay mold of each section to obtain a cross-sectional image of the shape of that part of the tree at the height of the section. By referring to a scale included in each photograph, we determined the actual area (m²) of each pixel in the photograph, and we calculated the area of the cross-section by counting the number of pixels in the cross-section and multiplying it by the actual per pixel area. Then, by multiplying the cross-sectional area by 0.30 m (the measurement interval), we obtained the volume of each 0.30-m section of the stem and branch. For direct measurement of small branches, we used a cherry picker to cut out small branches that were distributed on the tree between heights of 10.00 and 11.00 m. Altogether, we cut out about 400 samples of small branches. We then submerged these small branches, which were each about 1 m long, in a water tank and obtained their volume by measuring the increase in the water volume. Since the volume was quickly measured, the influence of water permeation into the branches

on the volume estimation was negligible. We also measured the diameters of the sampled small branches at 100 randomly selected points with calipers and calculated the mean diameter at those points.

2.4. 3-D modeling using the obtained lidar data

2.4.1. Registration and voxelization

The 3-D modeling procedure is diagrammed in Fig. 1. We registered the 3-D point cloud data obtained at the six measurement points by the portable ground-based lidar systems into a common coordinate system by using the iterative closest-point algorithm (Besl and McKay, 1992). The error of the registration was within 2 cm. We then converted all points in the registered data set into voxel coordinates (Hosoi and Omasa, 2006). For the voxelization (i.e., conversion of the lidar-derived point-cloud data into volume elements in a 3-D array set in the computer memory), it is important for the voxel size to be determined appropriately; it must be small enough to adequately represent the lidar data as voxels. Therefore, we based the voxel size on the diameter of the small branches of the target tree because they are the thinnest parts of the target. The small-branch diameters were less than the lidar's laser beam pitch. Thus, a certain portion of a small branch hit by one laser beam was recorded as a lidar data point, and the portion of the small branch hit by one laser beam could be considered to be a cylinder with its height equal to the laser beam diameter (Fig. 2). We calculated the volume of the cylinder from the mean laser beam diameter (1.2 cm) and the mean small-branch diameter (0.37 cm; obtained as described in Section 2.3 of the Methods) to be 0.13 cm³. Then we chose the voxel size so that its volume would be approximately the same as that of the cylinder, that is, 0.5 cm × 0.5 cm × 0.5 cm. We thus produced our initial 3-D voxel-based model of the zelkova tree using voxels of that size.
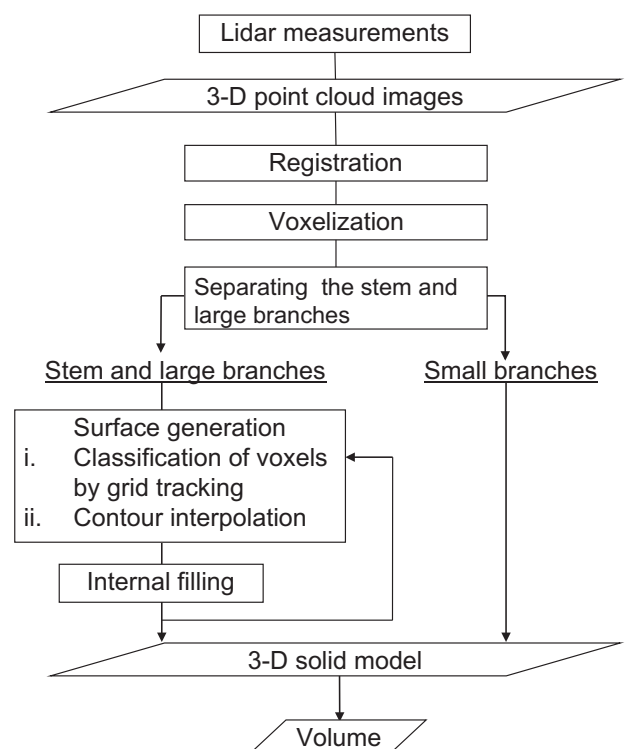

Fig. 1. Schematic diagram of 3-D voxel-based solid tree modeling from portable scanning lidar measurements.
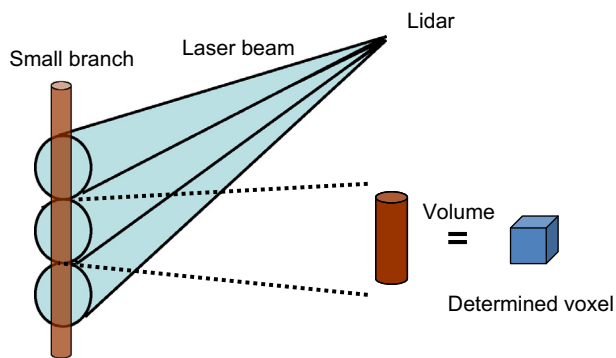
Fig. 2. Determination of voxel size. The voxel dimensions were selected so that the volume of one voxel would be the same as the volume of the portion of a small branch irradiated by one laser beam.

2.4.2. Separating the stem and large branches from small branches

After the initial voxelization of the target, we needed to separate the voxels of the stem and larger branches from those of the small branches for further characterization ("Separating the stem and large branches" in Fig. 1). First, we manually picked several voxels corresponding to the stem or large branches from the voxelized 3-D model. We used these as starting points for separating the stem and large branches from small branches. Then, we categorized voxels neighboring these initial voxels within a certain distance (in this case, 1 cm) as stem or large-branch voxels. The categorized voxels then became new initial (starting) points and the above searching procedure was repeated. This procedure was iterated until no more voxels could be categorized as stem or large branches. Then, we categorized all of the remaining voxels as small-branch voxels.

2.4.3. Surface generation

We applied a surface generation procedure to the voxels categorized as stem or large-branch voxels ("Surface generation" in Fig. 1). The voxels converted from the lidar data on the surfaces of the stem and large branches were not adjacent because the laser beam pitch (mean = 1.2 cm) was larger than the pitch of the voxel array (0.5 cm). The surface generation procedure interpolated additional voxels between the initial voxels of each one-voxel-thick horizontal layer of the voxelized model to obtain a continuous closed curve representing the exterior surface of the stem and each large branch by the following two steps (Fig. 3).

2.4.3.1. Classification of voxels into sets, each representing either the stem or a large branch, by grid tracing.
To generate the surfaces, we first classified the voxels within a horizontal layer into sets, each one corresponding to the stem or to a large branch. To do this, we first superimposed a grid on each horizontal voxel layer. We chose the grid size (2 cm × 2 cm) to be larger than both the original voxels and the laser beam pitch (Fig. 3B). We then filled (labeled) each cell of the grid that included at least one voxel and used Moore's neighbor-tracing algorithm to connect adjacent filled cells to trace the approximate contour of the exterior surface of the stem or large branch (Ghuneim, 2009). In this method, cells in each row of the grid, starting from the top row and proceeding to the bottom row, were scanned from the leftmost to the rightmost. Then, the first-encountered filled cell was treated as a starting cell and the eight neighboring cells were examined in a clockwise direction until another filled cell was encountered; this encountered cell was then treated as the next cell in the contour. These steps were repeated until the starting cell was again encountered. This procedure yielded a closed curve outlining the stem or a large branch. During this procedure, the starting cell and each selected cell were labeled (a certain value was given to each cell as its attribute value), thus producing a set of labeled cells corresponding to the stem or to a large branch. Next, scanning of the grid was repeated, skipping already labeled cells, and the first-encountered filled and unlabeled cell was treated as the next starting cell. The same procedure was applied to the other filled cells, with different labels being used to discriminate the stem and each large branch (Fig. 3B: (a), (b), and (c)). In this way, we classified the voxels included in the cells into sets, each of which corresponded either to the stem or to a specific large branch.

2.4.3.2. Contour interpolation.
We next applied a contour interpolation procedure to each set of classified voxels (Fig. 3C) within a horizontal layer. Here, we no longer used the superimposed grid cells (2 cm × 2 cm) described above. To generate contours of the exterior surfaces of the stem and each large branch composed of consecutive voxels, gaps (empty voxels) between voxels in a voxel set were filled by linear interpolation. First, voxels that should not be included in a contour were excluded as noise (Fig. 3C). We judged whether a voxel was noise by calculating the mean (d_m) and standard deviation (σ) of the distance between each voxel and the centroid of the voxel set. We regarded voxels at a distance of more than $d_m + 3\sigma$ as noise and excluded them from the set. Next, we calculated the angle between the x-axis and each line segment connecting a voxel with the centroid of the voxel set. We then sorted the angles in ascending order to determine the tracking order of each voxel. Then, to generate the contour, we picked a certain tracked voxel and then filled the empty voxels between that voxel and the next filled voxel in the tracking order by linear interpolation (Fig. 3C). We repeated this procedure until all voxels composing the contour of the exterior surface of the stem or large branch had been filled (that is, until a continuous contour composed of consecutively filled voxels had been generated). This procedure was applied to each classified voxel set within a horizontal voxel layer and repeated from the lowest to the highest horizontal layer, thus generating exterior surfaces of the stem and each large branch composed of consecutive voxels.

2.4.4. Interior filling and generation of the 3-D voxel-based solid model

We filled the interiors of the stem and each large branch by scanning between the voxels of a contour in both the x and y directions (Fig. 3D). For instance, for a scan in the x direction, we picked a starting voxel near the lower left of the contour and traced a line in the positive x direction from the starting voxel to the voxel on the opposite side of the contour. The first voxel was equivalent to the minimum and the last voxel to the maximum x-coordinate value along the scan line, and all empty voxels between the starting and ending voxels were labeled. We repeated this procedure for each voxel along the contour in both the x and y directions. Then, we regarded those voxels that had been labeled twice (that is, by both the x- and y-direction scans) as interior voxels of that contour and filled them. We applied this interior filling procedure to the stem and all large branches within each horizontal voxel layer, from the lowest to the highest horizontal layer. In this way, we filled both the surfaces and interiors of the entire stem and all large branches with consecutive voxels. We then produced a 3-D voxel-based solid model of the whole target tree by merging the filled stem and large branches with the voxels previously categorized into small branches (Section 2.4.2).

2.5. Estimation of woody material volume from the 3-D solid model

We calculated the volume of the woody material from the generated 3-D voxel-based solid model. This model was composed of consecutive voxels that filled the outer surfaces and the interiors of the stem and large branches, and a cloud of voxels equivalent
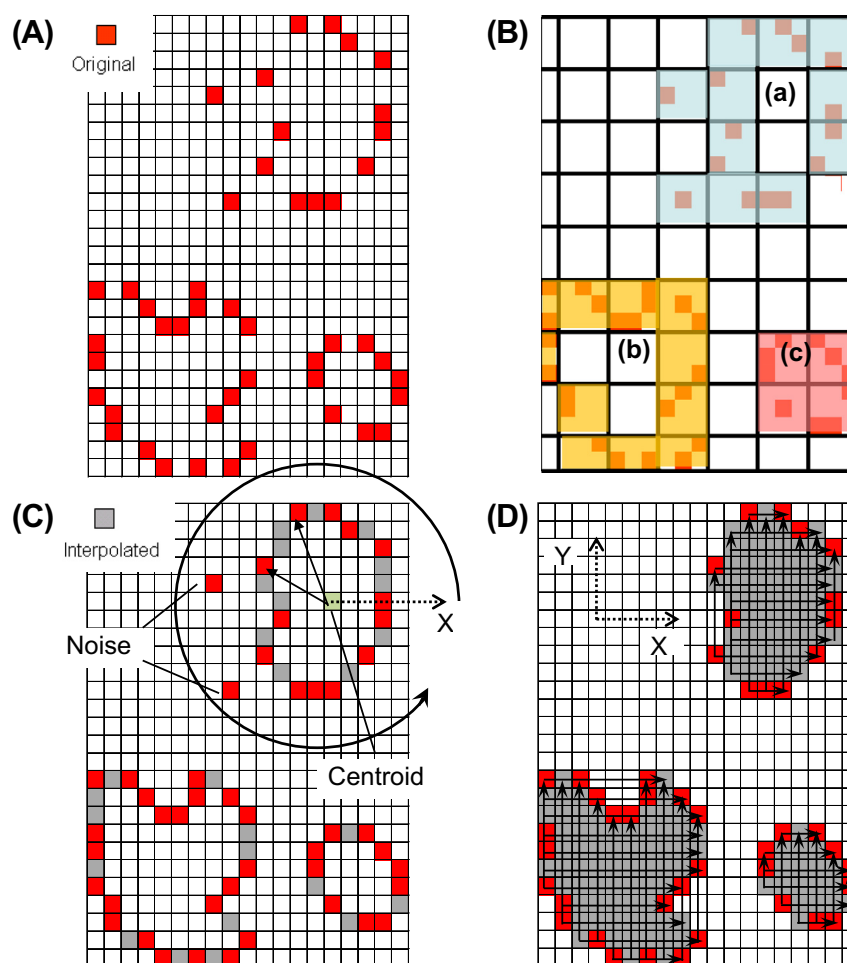
Fig. 3. Generation of the exterior surface contours of the stem and large branches. (A) Original voxels (dark gray in the print version, red in the online version) within a horizontal layer obtained by conversion of the lidar data points. (B) A grid was overlaid on a one-voxel-thick horizontal layer, and voxel sets (a), (b), and (c), corresponding to the contours of the stem and each large branch (hatched or gray colored in the print version, light blue, yellow, and pink colored in the online version), were identified by connecting cells using a neighbor-tracing algorithm. (C) Contours of the stem and of large branches were filled by interpolating voxels (light gray) between the original voxels (dark gray in the print version, red in the online version). Original voxels too far from the centroid of each voxel set were excluded as noise. (D) Interior voxels were identified and filled by scanning in the *x* and *y* directions from voxels on the contour.

to small branches that were discretely scattered in mainly the upper part of the target. By using the model, we could easily estimate the woody material volume of any part of the tree by counting the number of voxels within the part and then multiplying the number of voxels by the unit voxel volume ($0.5 \times 0.5 \times 0.5 \approx 0.13 \text{ cm}^3$). In the present study, we calculated the volumes of the stem and large and small branches within each 1.00-m-thick horizontal layer to determine the vertical distribution of volume within the target. Then, we summed the volumes in each layer to obtain the total stem and large-branch volume, the total small-branch volume, and the whole woody material volume. Also, to validate the volume estimation, we extracted the part of the tree chosen for direct measurement (see Section 2.3) from the model and determined its volume separately. Then we compared the model estimation with the directly measured volume to obtain the estimation error.

3. Results

The 3-D voxel-based solid model of the zelkova tree generated from the 3-D point cloud data obtained by the portable scanning lidar system faithfully reproduced each part of the target because of the fine resolution of the lidar image and appropriate setting of the voxel size (Fig. 4B). The small branches were well separated

from the stem and large branches, and a cross-sectional view of the stem shows that both the outer surface of the model and its interior are composed of consecutively filled voxels (Fig. 4C).

Examination of the estimated volume at each height (Fig. 5) showed that the volume of the stem and large branches increased as the height decreased, reaching its maximum in the lowest height interval (Fig. 5). Conversely, the volume of the small branches increased with height and reached its maximum value at 12.00 m. As a result, between heights of 0.00 and 9.00 m, most of the total volume was accounted for by the stem and large branches, but above 9.00 m height, most of the volume was in small branches. In the whole target, the volume of the stem and large branches was 0.417 m³, and that of the small branches was 0.135 m³, for a total volume of 0.552 m³ for the whole target.

Direct stem and branch measurements (Fig. 6A) and model-estimated stem and branch volume demonstrated strong agreement (Fig. 6B). The mean absolute percentage error, obtained by calculating the absolute percentage error in each height interval and then averaging them, was 6.8%. The error of the total volume of the part, obtained by summing the volumes of each height interval, was 0.5%. The estimated percentage error corresponding to the sampled part of the small branches, obtained by comparing the estimated volume with the directly measured value, was 34.0%.
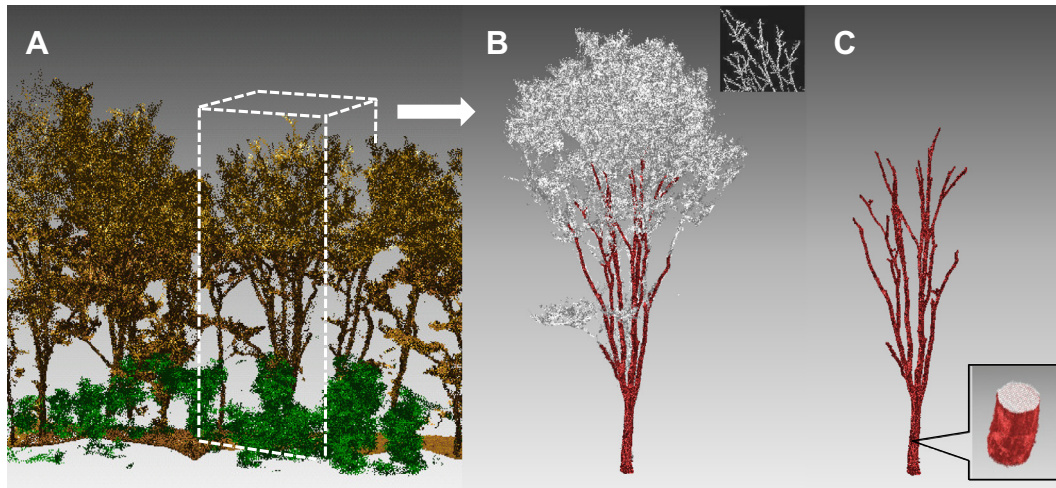
Fig. 4. The 3-D voxel-based solid model of the zelkova tree generated from the 3-D point cloud data obtained by portable scanning lidar. (A) A point cloud image of a group of zelkova trees before voxelization. Area enclosed by dashed lines is the target tree within the measurement plot (the evergreen understory is colored green in the online version). (B) The 3-D model of the target tree: small branches are white. The upper-right figure is a close-up view of small branches in the model. (C) Stem and large branches only. In the cross-section of a part of the stem, the interior voxels are colored white.
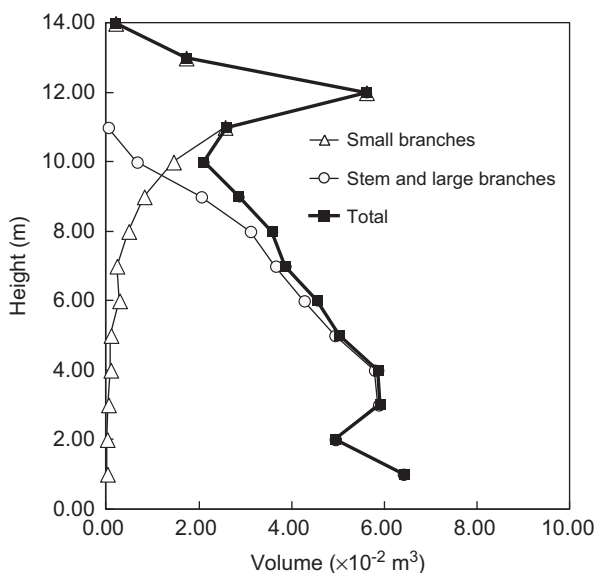

Fig. 5. The estimated volume of the stem and large branches, the estimated volume of the small branches, and the estimated total volume, derived from the voxel-based solid model by counting voxels in each 1.0-m height interval.

4. Discussion

Our results demonstrated that a 3-D voxel solid tree model based on portable scanning lidar data can accurately capture the complex structure of an individual tree. In this method, we used lidar data obtained by fully illuminating the target with high-pulse-density laser beams emitted from multiple measurement positions surrounding the target to reproduce the complex shape of the target with consecutive voxels, thus producing an accurate model. No approximation of tree shape is required by this method, such as the approximation of the stem and large branch as cylinders in some previously proposed volume estimation methods (Côté et al., 2009, 2011; Delagrange and Rochon, 2011; Lefsky and McHale, 2008). Such approximation causes errors when the shapes of the stem and large branches are complex, whereas the present method can accurately estimate the volumes iof stems and large branches with complex shapes that are quite different from

cylinders. The accuracy of the model based on the present method also depends on the voxel size used. In particular, because small branches are very thin, the estimation of their volume might include an error if the voxel size is not fine enough. In a recent study, Vonderach et al. (2012) estimated tree volume by counting the number of voxels after using portable scanning lidar data to voxelize the target trees. However, they used larger voxels ($1 \text{ cm} \times 1 \text{ cm} \times 1 \text{ cm}$) so that the voxels would be adjacent. As Vonderach et al. (2012) noted, the use of large voxels caused the volume of small branches in particular to be overestimated and also was less suitable for expressing the complex shapes of the stem and branches. Here, we chose the voxel size so that the volume of a voxel would be the same as that of the portion of a small branch hit by a single laser beam. This smaller voxel size prevented the overestimation reported by Vonderach et al. (2012) and allowed the complex shape of the target tree to be faithfully reproduced. Although we directly measured the diameters of small branches by destructive sampling for voxel size determination, easier measurement methods need to be devised to improve the general applicability of our method to various species.

Previous studies have used voxel representations of a tree canopy for estimating leaf area density profiles by the Voxel-based Canopy Profiling method, in which voxels are used to trace laser beams for calculating the contact frequency of laser beams on the canopy (Hosoi and Omasa, 2006, 2007, 2009, 2012; Hosoi et al., 2010; Omasa et al., 2007). In contrast, in this study, we used voxels to reproduce the woody material of the target tree as a solid model for estimating woody material volume, so the present method should be distinguished from the Voxel-based Canopy Profiling method.

In the voxelization process, voxels belonging to the stem and large branches needed to be separated from those of the small branches because additional procedures must be applied to obtain the volumes of the stem and large branches. We used the difference in spatial distribution between the voxels of the stem and large branches and those of the small branches to achieve this separation. Because the stem and large branches are wider than the laser beam's pitch, the voxels on their surfaces are arranged relatively regularly according to the laser beam pitch. As a result, voxels corresponding to the stem and large branches can be extracted by searching for voxels within a certain distance (here, set to 1 cm, which is approximately equivalent to the laser beam pitch) from initial voxels picked from the stem and large branches.
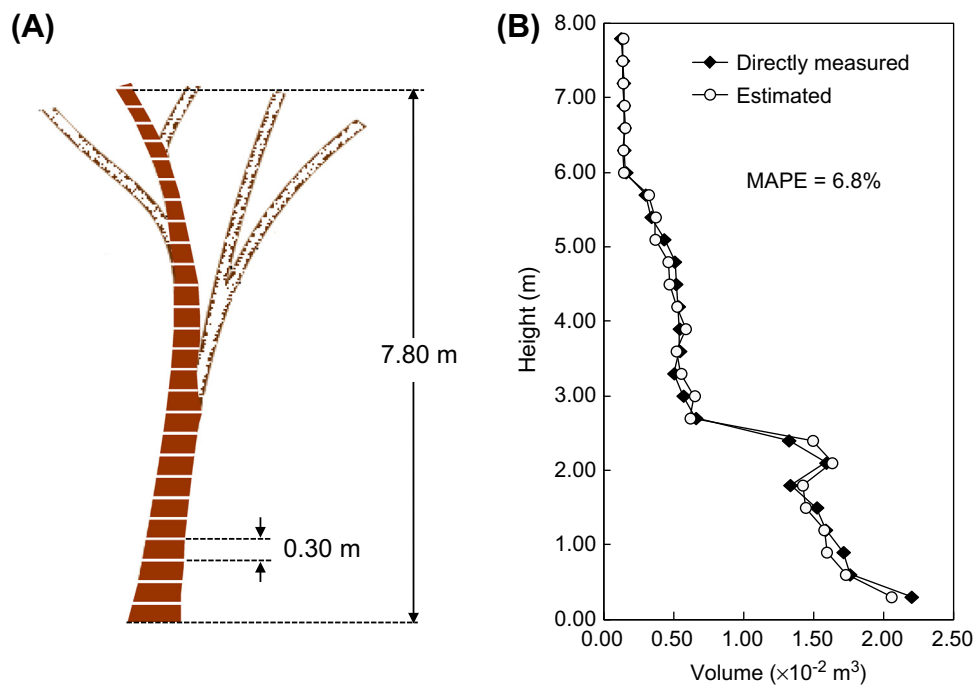
Fig. 6. Comparison of the woody material volume estimated from the voxel solid model and the directly measured volume for each 0.30-m height interval. (A) The part of the target tree chosen for direct measurement (gray part in the print version, brown part in the online version). (B) Vertical distributions of the estimated and directly measured volumes. MAPE, mean absolute percentage error.

In contrast, because the diameter of a small branch is smaller than the laser beam's pitch, voxels on small branches are not regularly distributed regardless of the laser beam pitch. The nearest-neighbor distances of most of these voxels were larger than those of the stem and large branches, so most small branch voxels were not extracted along with the stem and large branch voxels.

To classify the voxels within a horizontal layer into sets so that each set would correspond to the stem or to a large branch, we utilized the contours of the stem and large branches. Those voxels included in the same contour were judged as belonging to the same stem or branch. To support this judgment, we applied a neighbor-tracing algorithm (Ghuneim, 2009) to each horizontal layer of voxels. This algorithm requires consecutively connected pixels on a closed curve, but the equivalent voxels on each of the surface contours of the stem and large branches were not consecutively connected. To satisfy this requirement, therefore, we overlaid a grid on each horizontal layer. Since the size of the cells in the grid was larger than the laser beam's pitch, neighboring cells were consecutive, allowing application of the neighbor-tracing algorithm and classification of the voxels.

We then used linear interpolation to label all voxels along the exterior surface contours of the stem and each large branch. Although each contour was a curved line, linear interpolation could reproduce the contour because of the high laser pulse density of the lidar measurements. We obtained this high density by adjusting the laser beam pitch and by taking measurements from several points around the target. As a result, many voxels lay on each contour and distances between neighboring voxels were short. Thus, lidar measurements must be made with high laser pulse density for accurate 3-D modeling of a tree. It might be difficult to obtain an adequately high laser pulse density, depending on the conditions at the study site. In that case, the voxels would be sparsely distributed along each contour and a non-linear interpolation method, for example, spline interpolation, might be more appropriate than linear interpolation.

The estimation error for the small branches was higher than that for the stem and large branches. In the upper part of the target,

where there were a great many, intricately branched small branches, some small branches were probably not illuminated by the laser beams because they were obstructed by other small branches. The obstruction effect is a major problem with the other 3-D tree modeling methods based on portable scanning lidar data (Dassot et al., 2011). For example, underestimation of tree biomass by the tree skeleton extraction method has been attributed to partial occlusion of the inner parts of branches within the crown (Delagrange and Rochon, 2011). In addition, because the small branches are very thin, the intensity of some of the returned laser beams might have been too low to be detected by the lidar sensor. This loss of information about the small branches probably increased the error. A different laser beam diameter setting or the use of additional measurement positions might improve the accuracy of our method. Multi-return or waveform-recording ground-based lidar systems (Strahler et al., 2008; Yao et al., 2011) might also be able to extract more information about the small branches.

In this study, we aimed to establish the basic principles of solid tree modeling based on lidar-derived data. Therefore, we targeted a relatively narrow area that included just one tree and used a portable scanning lidar with a relatively short measurable range. The present method could be applied to a larger area that includes more trees by using a portable scanning lidar with a longer measurable range and by establishing more measurement positions. Although the multiple scans needed in the present method may cause the measurement time to be long, the measurement time could be shortened by using one of the currently available portable scanning lidars capable of high-speed scanning.

The solid model obtained with our method faithfully retains spatial information contained in the raw 3-D point cloud data provided by the portable scanning lidar. Thus, it would also be possible to extract other structural parameters besides woody material volume, such as tree height and stem diameter, from the lidar-derived 3-D point cloud data by using previously proposed methods (Hopkinson et al., 2004; Omasa et al., 2002). This characteristic is an important advantage of our method over conventional tree modeling methods.

5. Conclusions

In this study, we demonstrated a method to produce a 3-D voxel-based solid model of the tree from portable scanning lidar data that allows accurate volume estimation. The present method utilizes almost all spatial information contained in the lidar-derived 3-D point cloud data to model the complex shape of the target. One advantage of this volume estimation method compared with other methods that use allometric equations or approximations of stem and branch shapes is that no allometric equations are needed and shapes are not approximated. By using the model, the woody material volume of not only the whole target tree but also of any part of the target tree can be directly calculated easily and accurately by counting the number of corresponding voxels and multiplying the result by the per-voxel volume. The overall accuracy of the volume estimation results using the model was satisfactory, as confirmed by comparing the volume estimates with directly measured volumes. Future studies should investigate the applicability of the method to larger regions with different conditions and species, using portable scanning lidar systems with different performance and considering measurement settings such as the number of scans and the distance between the target and lidar positions.

References

Besl, P.J., McKay, N.D., 1992. A method for registration of 3-D shapes. IEEE Transactions on Pattern Analysis and Machine Intelligence 14 (2), 239–256.

Bragg, D.C., 2008. An improved tree height measurement technique tested on mature southern pines. Southern Journal of Applied Forestry 32 (1), 38–43.

Brandtberg, T., Warner, T.A., Landenberger, R.E., McGraw, J.B., 2003. Detection and analysis of individual leaf-off tree crowns in small footprint, high sampling density lidar data from the eastern deciduous forest in North America. Remote Sensing of Environment 85 (3), 290–303.

Bucksch, A., Lindenbergh, R., 2008. CAMPINO—a skeletonization method for point cloud processing. ISRPS Journal of Photogrammetry and Remote Sensing 63 (1), 115–127.

Côté, J.F., Fournier, R.A., Egli, R., 2011. An architectural model of trees to estimate forest structural attributes using terrestrial LiDAR. Environmental Modeling and Software 26 (6), 761–777.

Côté, J.F., Widlowski, J.L., Fournier, R.A., Verstraete, M.M., 2009. The structural and radiative consistency of three-dimensional tree reconstructions from terrestrial lidar. Remote Sensing of Environment 113 (5), 1067–1081. http://dx.doi.org/10.1016/j.rse.2009.01.017.

Dassot, M., Constant, T., Fournier, M., 2011. The use of terrestrial LiDAR technology in forest science: application fields, benefits and challenges. Annals of Forest Science 68 (5), 959–974.

Delagrange, S., Rochon, P., 2011. Reconstruction and analysis of a deciduous sapling using digital photographs or terrestrial-LiDAR technology. Annals of Botany 108 (6), 991–1000.

Ghuneim, A.G., 2009. Moore-Neighbor Tracing Idea. <http://www.imageprocessingplace.com/downloads_V3/root_downloads/tutorials/contour_tracing_Abeer_George_Ghuneim/moore.html>.

Holmgren, J., Persson, Å., 2004. Identifying species of individual trees using airborne laser scanner. Remote Sensing of Environment 90 (4), 415–423.

Hopkinson, C., Chasmer, L., Young-Pow, C., Treitz, P., 2004. Assessing forest metrics with a ground-based scanning lidar. Canadian Journal of Forest Research 34 (3), 573–583. http://dx.doi.org/10.1139/X03-225.

Hosoi, F., Nakai, Y., Omasa, K., 2010. Estimation and error analysis of woody canopy leaf area density profiles using 3-D airborne and ground-based scanning lidar remote-sensing techniques. IEEE Transactions on Geoscience and Remote Sensing 48 (5), 2215–2223.

Hosoi, F., Omasa, K., 2006. Voxel-based 3-D modeling of individual trees for estimating leaf area density using high-resolution portable scanning lidar. IEEE Transactions on Geoscience and Remote Sensing 44 (12), 3610–3618.

Hosoi, F., Omasa, K., 2007. Factors contributing to accuracy in the estimation of the woody canopy leaf-area-density profile using 3D portable lidar imaging. Journal of Experimental Botany 58 (12), 3464–3473.

Hosoi, F., Omasa, K., 2009. Estimating vertical plant area density profile and growth parameters of a wheat canopy at different growth stages using three-dimensional portable lidar imaging. ISRPS Journal of Photogrammetry and Remote Sensing 64 (2), 151–158.

Hosoi, F., Omasa, K., 2012. Estimation of vertical plant area density profiles in a rice canopy at different growth stages by high-resolution portable scanning lidar with a lightweight mirror. ISRPS Journal of Photogrammetry and Remote Sensing 74, 11–19.

Hyyppä, J., Kelle, O., Lehikoinen, M., Inkinen, M., 2001. A segmentation-based method to retrieve stem volume estimates from 3-D tree height models produced by laser scanners. IEEE Transactions on Geoscience and Remote Sensing 39 (5), 969–975.

Jones, H.G., 1992. Plants and Microclimate, second ed. Cambridge University Press, Cambridge.

Kaartinen, H., Hyyppä, J., Yu, X.W., Vastaranta, M., Hyyppä, H., Kukko, A., Holopainen, M., Heipke, C., Hirschmugl, M., Morsdorf, F., Næsset, E., Pitkänen, J., Popescu, S., Solberg, S., Wolf, B.M., Wu, J.C., 2012. An international comparison of individual tree detection and extraction using airborne laser scanning. Remote Sensing 4 (4), 950–974.

Ku, N.W., Popescu, S.C., Ansley, R.J., Perotto-Baldivieso, H.L., Filippi, A.M., 2012. Assessment of available rangeland woody plant biomass with a terrestrial lidar system. Photogrammetric Engineering and Remote Sensing 78 (4), 349–361.

Larcher, W., 2001. Physiological Plant Ecology, fourth ed. Springer, Heidelberg.

Lefsky, M.A., Cohen, W.B., Parker, G.G., Harding, D.J., 2002. Lidar remote sensing for ecosystem studies. Bioscience 52 (1), 19–30.

Lefsky, M., McHale, M., 2008. Volume estimates of trees with complex architecture from terrestrial laser scanning. Journal of Applied Remote Sensing 2. http://dx.doi.org/10.1117/1.2939008.

le Maire, G., Marsden, C., Nouvellon, Y., Grinand, C., Hakamada, R., Stape, J.L., Laclac, J.P., 2011. MODIS NDVI time-series allow the monitoring of *Eucalyptus* plantation biomass. Remote Sensing of Environment 115 (10), 2613–2625.

Maselli, F., Marta, C., 2006. Evaluation of statistical methods to estimate forest volume in a Mediterranean region. IEEE Transactions on Geoscience and Remote Sensing 44 (8), 2239–2250.

Means, J.E., Acker, S.A., Harding, D.J., Blair, J.B., Lefsky, M.A., Cohen, W.B., Harmon, M.E., McKee, W.A., 1999. Use of large-footprint scanning airborne lidar to estimate forest stand characteristics in the Western Cascades of Oregon. Remote Sensing of Environment 67 (3), 298–308.

Monteith, J.L., 1973. Principles of Environmental Physics. Edward Arnold, London.

MobileReference, 2009. The Illustrated Encyclopedia of Trees and Shrubs: An Essential Guide to Trees and Shrubs of the World. MobileReference, Boston.

Næsset, E., Gobakken, T., Holmgren, J., Hyyppä, H., Hyyppä, J., Maltamo, M., Nilsson, M., Olsson, H., Persson, Å., Söderman, U., 2004. Laser scanning of forest resources: the Nordic experience. Scandinavian Journal of Forest Research 19 (6), 482–499.

Neumann, M., Saatchi, S.S., Ulander, L.M.H., Fransson, J.E.S., 2012. Assessing performance of L- and P-band polarimetric interferometric SAR data in estimating boreal forest above-ground biomass. IEEE Transactions on Geoscience and Remote Sensing 50 (3), 714–726.

Norman, J.M., Campbell, G.S., 1989. Canopy structure. In: Pearcy, R.W., Ehleringer, J., Mooney, H.A., Rundel, P.W. (Eds.), Plant physiological Ecology: Field Methods and Instrumentation. Chapman and Hall, London, pp. 301–325.

Omasa, K., Akiyama, Y., Ishigami, Y., Yoshimi, K., 2000. 3-D remote sensing of woody canopy heights using a scanning helicopter-borne lidar system with high spatial resolution. Journal of Remote Sensing Society of Japan 20 (4), 394–406.

Omasa, K., Urano, Y., Oguma, H., Fujinuma, Y., 2002. Mapping of tree position of *Larix leptolepis* woods and estimation of diameter at breast height (DBH) and biomass of the trees using range data measured by a portable scanning lidar. Journal of Remote Sensing Society of Japan 22 (5), 550–557.

Omasa, K., Qiu, G.Y., Watanuki, K., Yoshimi, K., Akiyama, Y., 2003. Accurate estimation of forest carbon stocks by 3-D remote sensing of individual trees. Environmental Science and Technology 37 (6), 1198–1201.

Omasa, K., Hosoi, F., Konishi, A., 2007. 3D lidar imaging for detecting and understanding plant responses and canopy structure. Journal of Experimental Botany 58 (4), 881–898.

Omasa, K., Hosoi, F., Uenishi, T.M., Shimizu, Y., Akiyama, Y., 2008. Three-dimensional modelling of an urban park and trees by combined airborne and portable on-ground scanning LIDAR remote sensing. Environmental Modeling and Assessment. http://dx.doi.org/10.1007/s10666-007-9115-5.

Pirotti, F., Guarnieri, A., Vettore, A., 2013. State of the art of ground and aerial laser scanning technologies for high-resolution topography of the earth surface. European Journal of Remote Sensing 46, 66–78.

Schilling, A., Schmidt, A., Maas, H.G., 2012. Tree topology representation from TLS point clouds using depth-first search in voxel space. Photogrammetric Engineering and Remote Sensing 78 (4), 383–392.

Schnitzer, S.A., DeWalt, S.J., Chave, J., 2006. Censusing and measuring lianas: a quantitative comparison of the common methods. Biotropica 38 (5), 581–591.

Strahler, A.H., Jupp, D.L.B., Woodcock, C.E., Schaaf, C.B., Yao, T., Zhao, F., Yang, X., Lovell, J., Culvenor, D., Newnham, G., Ni-Miester, W., Boykin-Morris, W., 2008. Retrieval of forest structural parameters using a ground-based lidar instrument (Echidna®). Canadian Journal of Remote Sensing 34 (2), 426–440.

Vonderach, C., Vögtle, T., Adler, P., Norra, S., 2012. Terrestrial laser scanning for estimating urban tree volume and carbon content. International Journal of Remote Sensing 33 (21), 6652–6667.

Yao, T., Yang, X., Zhao, F., Wang, Z., Zhang, Q., Jupp, D., Lovell, J., Culvenor, D., Newnham, G., Ni-Meister, W., Schaaf, C., Woodcock, C., Wang, J., Li, X., Strahler, A., 2011. Measuring forest structure and biomass in New England forest stands using Echidna ground based lidar. Remote Sensing of Environment 115 (11), 2965–2974.

Zhao, K., Popescu, S., Meng, X., Pang, Y., Agca, M., 2011. Characterizing forest canopy structure with lidar composite metrics and machine learning. Remote Sensing of Environment 115 (8), 1978–1996.